Impact Ionization Coefficients of Digital Alloy and Random Alloy $Al_{0.85}Ga_{0.15}As_{0.56}Sb_{0.44}$ in a Wide Electric Field Range

Bingtian Guo, Xiao Jin, Seunghyun Lee, Sheikh Z. Ahmed, Andrew H. Jones, Xingjun Xue, Baolai Liang, Harry I. J. Lewis, Sri H. Kodati, Dekang Chen, Theodore J. Ronningen, Christoph H. Grein, Avik W. Ghosh, *Senior Member, IEEE*, Sanjay Krishna, *Fellow, IEEE*, John P. R. David, *Fellow, IEEE*, and Joe C. Campbell, *Life Fellow, IEEE*

***Abstract*—Digital alloy and random alloy $Al_{0.85}Ga_{0.15}As_{0.56}Sb_{0.44}$ avalanche photodiodes (APDs) exhibit low excess noise, comparable to Si APDs. Consequently, this material is a promising multiplication layer candidate for separate absorption, charge, and multiplication structure APDs with high gain-bandwidth product. Characterization of the impact ionization coefficients of electrons (α) and holes (β) plays an important role in the simulation of avalanche photodiodes. The multiplication gain curves of eight p^+-i-n^+ and n^+-i-p^+ APDs covering a wide range of avalanche widths have been used to determine the electric field dependence of the impact ionization coefficients of $Al_{0.85}Ga_{0.15}As_{0.56}Sb_{0.44}$. A large impact ionization coefficient ratio between that of electrons to holes was seen across a wide electric field range. Simulations of the avalanche multiplication in these structures using a random path length (RPL) model gave good agreement with experimental results over almost three orders of magnitude, and a mixed injection method was employed to verify the extracted impact ionization coefficients. Interestingly, no difference in the impact ionization coefficients was seen between digital alloy and random alloy $Al_{0.85}Ga_{0.15}As_{0.56}Sb_{0.44}$. This knowledge of impact ionization coefficients is beneficial for the future utilization of the $Al_xGa_{1-x}As_ySb_{1-y}$ material system.**

***Index Terms*—AlGaAsSb, avalanche photodiode, digital alloy, impact ionization coefficient, random alloy.**

Manuscript received February 16, 2022; revised March 30, 2022; accepted April 18, 2022. Date of publication April 22, 2022; date of current version July 16, 2022. The work of Harry I. J. Lewis was supported by the EPSRC Studentship under Grant EP/R513313/1. This work was supported by the Directed Energy–Joint Technology Office (DE-JTO) under Grant N00014-17-1-2440. (*Bingtian Guo and Xiao Jin are co-first authors.*) *(Corresponding author: Joe C. Campbell.)*

Bingtian Guo, Sheikh Z. Ahmed, Andrew H. Jones, Xingjun Xue, Dekang Chen, Avik W. Ghosh, and Joe C. Campbell are with the Department of Electrical and Computer Engineering, University of Virginia, Charlottesville, VA 22904 USA (e-mail: bg8ws@virginia.edu; sza9wz@virginia.edu; ahj2ge@virginia.edu; xingjunxue@gmail.com; dc5rc@virginia.edu; ag7rq@virginia.edu; jcc7s@virginia.edu).

Xiao Jin, Harry I. J. Lewis, and John P. R. David are with the Department of Electronic and Electrical Engineering, University of Sheffield, S1 3JD Sheffield, U.K. (e-mail: xjin4@sheffield.ac.uk; hlewis2@sheffield.ac.uk; j.p.david@sheffield.ac.uk).

Seunghyun Lee, Sri H. Kodati, Theodore J. Ronningen, and Sanjay Krishna are with the Department of Electrical and Computer Engineering, The Ohio State University, Columbus, OH 43210 USA (e-mail: lee.8014@buckeyemail.osu.edu; kodati.2@buckeyemail.osu.edu; ronningen.1@osu.edu; krishna.53@osu.edu).

Baolai Liang is with the California NanoSystems Institute, University of California, Los Angeles, CA 90095 USA (e-mail: bliang@cnsi.ucla.edu).

Christoph H. Grein is with the Department of Physics, University of Illinois, Chicago, IL 60607 USA (e-mail: grein@uic.edu).

Color versions of one or more figures in this article are available at https://doi.org/10.1109/JLT.2022.3169008.

Digital Object Identifier 10.1109/JLT.2022.3169008

I. Introduction

AVALANCHE photodiodes (APDs) have been widely used in commercial, research, and military applications including imaging, optical communications, and single photon detection [1], [2]. Their internal gain enables higher receiver sensitivity than p-i-n photodiodes. The internal gain originates from serial impact ionization, a random process that also introduces noise which is characterized by introducing a multiplicative excess noise factor *F(M)* into the expression for the shot noise current [3], [4]

$$\left\langle i_{\text{shot}}^2 \right\rangle = 2q\left(I_{\text{photo}} + I_{\text{dark}}\right)\left\langle M\right\rangle^2 F\left(M\right)\Delta f, \tag{1}$$

where q is the electric charge, I_{photo} is the photocurrent, I_{dark} is the dark current, $<M>$ is the average gain, and Δf is the bandwidth. The excess noise factor can be expressed as [5]

$$F\left(M\right) = k\left\langle M\right\rangle + (1-k)\left(2 - \frac{1}{\left\langle M\right\rangle}\right), \tag{2}$$

where k is the ratio of the impact ionization coefficients of holes (β) to electrons (α) for the electron-initiated impact ionization process. They represent a carrier's mean rate of ionization per unit distance and are also equal to the inverse of the mean distance a carrier travels before ionizing. The excess noise factor increases with gain, but the rate of increase is lower for a material with a lower k-value. Therefore, the higher the gain the higher the excess noise, resulting in a higher total noise. The tradeoff between the receiver circuit noise suppression as a result of the intrinsic APD gain and the concomitant increasing shot and excess noise can be expressed by the signal to noise ratio (SNR),

$$SNR = \frac{I_{\text{photo}}^2}{2q\left(I_{\text{photo}} + I_{\text{dark}}\right)F\left(M\right)\Delta f + \frac{\sigma_{\text{circuit}}^2}{\left\langle M\right\rangle^2}}, \tag{3}$$

where σ_{circuit} is the RMS receiver circuit noise. Since the receiver circuit noise is non-negligible and unavoidable, the benefit of the APD internal gain can be maximized by a lower excess noise factor, i.e., a lower *k*-value, ultimately resulting in higher receiver sensitivity.

Recently, APDs based on $Al_xIn_{1-x}As_ySb_{1-y}$ and $Al_xGa_{1-x}As_ySb_{1-y}$ materials systems [2] have exhibited low excess noise comparable to that of Si ($k \sim 0.01$) [6], [7]. $Al_xIn_{1-x}As_ySb_{1-y}$ APDs grown on GaSb as a digital alloy with x = 0.5, 0.6, and 0.7 were reported with *k* values as low as 0.01 [8]. Likewise, random alloy $Al_{0.79}In_{0.21}As_{0.74}Sb_{0.26}$ APDs on InP have shown a *k* value of 0.02 [9]. Digital alloy $AlAs_{0.56}Sb_{0.44}$ APDs on InP were reported with a *k* value of 0.005 [10]. However, $AlAs_{0.56}Sb_{0.44}$ APDs on InP have oxidization issues due to the high Al content, leading to a high surface dark current [11]. In order to mitigate this oxidization issue, Ga was incorporated, resulting in $Al_{0.85}Ga_{0.15}As_{0.56}Sb_{0.44}$ APDs [11]–[16]. The digital alloy $Al_{0.85}Ga_{0.15}As_{0.56}Sb_{0.44}$ APDs, with a 1-μm multiplication layer, have shown a dark current which is approximately two orders of magnitude lower than $AlAs_{0.56}Sb_{0.44}$ APDs [14]. Both these Sb-based materials systems are promising candidates for low-noise APD multiplication layers.

In this work, the gain characteristics of two digital alloy (DA) and six random alloy (RA) $Al_{0.85}Ga_{0.15}As_{0.56}Sb_{0.44}$ (hereafter AlGaAsSb) APDs with different multiplication layer thickness were used to determine the electron and hole ionization coefficients of the AlGaAsSb over a wide electric field range. The electric field dependent impact ionization coefficients were extracted from these gain characteristics using a "local" model where the carrier ionization is assumed to be only a function of the electric field at that point [17]–[19], and no allowance is made for any "dead-space" [20] or history dependence of the carrier energy [21]. The experimental gain curves of p^+-i-n^+ and n^+-i-p^+ APDs under pure electron and hole injection profiles respectively were compared to simulations of the multiplication using these impact ionization coefficients. The extracted impact ionization coefficients were further verified through a mixed injection method [22] where the multiplication occurs due to the creation of electrons and holes within the depletion region of the p^+-i-n^+ APDs. The determination of impact ionization coefficients for AlGaAsSb is beneficial for the future design of high gain-bandwidth-product and low-noise separate absorption, charge, and multiplication (SACM) APDs [23]; it is also advantageous for the understanding of the physical mechanisms that contribute to low noise in Sb-based APDs.

II. Epitaxial Crystal Growth and Device Fabrication

The APDs were grown as p^+-i-n^+ and n^+-i-p^+ structures with different multiplication layer thickness on semi-insulating InP substrates by molecular beam epitaxy. The epitaxial structures are shown in Table I, and APDs with symmetrical p^+-i-n^+ and n^+-i-p^+ structures are listed in the same row. The multiplication layer thickness ranges from 87 nm to 1 μm with the growth details of some layers provided previously [13]–[16]. Doping and thickness of various layers shown in Table I were either taken from capacitance-voltage (C-V) measurements or the literature [13]–[16]. All samples employ InGaAs as the contact layer material, and their p-type and n-type layers were doped with Be and Si (or Te), respectively. With the exception of the 890-nm thick p^+-i-n^+ and n^+-i-p^+ multiplication layer structures which were grown as digital alloys [8], [10], [14], other samples in this study were grown as random alloys [11]–[13], [15], [16].

TABLE I
Epitaxial Structures of p^+-i-n^+ and n^+-i-p^+ AlGaAsSb APDs

Types	Material	Doping (cm^{-3})	Thickness (nm)
Random alloy p^+-i-n^+ (n^+-i-p^+) APDs [13]	InGaAs	p^{++} (n^{++})	100 (100)
	AlGaAsSb	p^+: 1.5×10^{18} (n^+: 2.4×10^{18})	300 (300)
	AlGaAsSb	UID	87 (98)
	AlGaAsSb	n^+: 1.5×10^{18} (p^+: 2.4×10^{18})	200 (200)
	InGaAs	n^{++} (p^{++})	1000 (1000)
	Semi-insulating InP substrate		
Random alloy p^+-i-n^+ (n^+-i-p^+) APDs [13]	InGaAs	p^{++} (n^{++})	100 (100)
	AlGaAsSb	p^+: 1.25×10^{18} (n^+: 2.4×10^{18})	300 (300)
	AlGaAsSb	UID	170 (193)
	AlGaAsSb	n^+: 1.25×10^{18} (p^+: 2.4×10^{18})	200 (200)
	InGaAs	n^{++} (p^{++})	1000 (1000)
	Semi-insulating InP substrate		
Digital alloy p^+-i-n^+ [14] (n^+-i-p^+) APDs	InGaAs	p^{++} (n^{++})	20 (20)
	AlGaAsSb	p^+: 1×10^{18} (n^+: 1×10^{18})	300 (300)
	AlGaAsSb	UID [1.5×10^{16} (1.9×10^{16})]	890 (890)
	AlGaAsSb	n^+: 1×10^{18} (p^+: 1×10^{18})	100 (100)
	InGaAs	n^{++} (p^{++})	400 (400)
	Semi-insulating InP substrate		
Random alloy p^+-i-n^+ APDs [15]	InGaAs	p^{++}	50
	AlGaAsSb	p^+: 1×10^{18}	300
	AlGaAsSb	UID [5×10^{15}]	608
	AlGaAsSb	n^+: 1×10^{18}	200
	InGaAs	n^{++}	500
	Semi-insulating InP substrate		
Random alloy p^+-i-n^+ APDs [16]	InGaAs	p^{++}	20
	AlGaAsSb	p^+: 1×10^{18}	300
	AlGaAsSb	UID [1×10^{15}]	1020
	AlGaAsSb	n^+: 1×10^{18}	100
	InGaAs	n^{++}	500
	Semi-insulating InP substrate		

The gain characteristics of the thinner structures have been reported previously [13], [15], so data from the literature was used in our analysis. For the three thickest samples, circular mesas were defined by UV lithography, and a solution of citric acid (10 g), phosphoric acid (6 mL), hydrogen peroxide (3 mL), and deionized water (60 mL) was used to chemically etch the mesas. Ti/Au contacts were deposited by electron-beam evaporation on the top and bottom InGaAs contact layers. Finally, SU-8 was spun on the sidewall to reduce the surface dark current.

III. Experiments and Results

A. Random Path Length Simulation

The current-voltage (I-V) characteristics of the three thickest AlGaAsSb p^+-i-n^+ and n^+-i-p^+ APDs measured at room temperature under dark and illuminated conditions were used

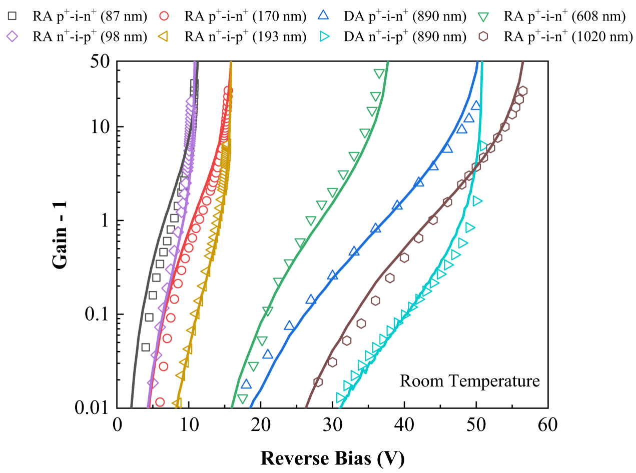

Fig. 1. Comparison between measured gain (symbols) under 450 nm illumination and simulated gain (solid lines) from the random path length model for p$^+$-i-n$^+$ and n$^+$-i-p$^+$ AlGaAsSb APDs with different multiplication layer thickness at room temperature.

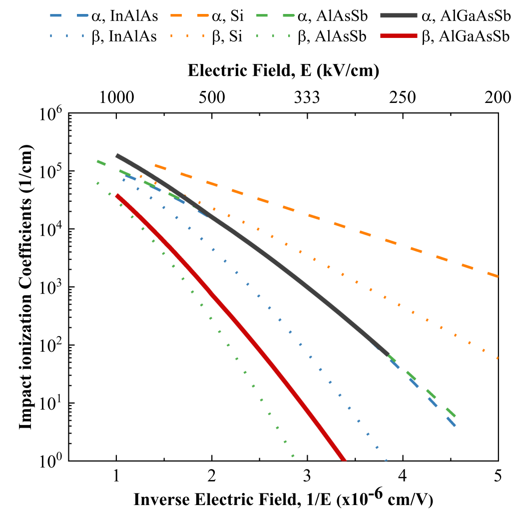

Fig. 2. Comparison of impact ionization coefficients of electrons and holes for AlGaAsSb, AlAsSb [26], Si [27], and InAlAs [28]. α of AlGaAsSb is similar to that of AlAsSb and InAlAs, and these lines overlap at low electric fields.

to determine the gain curves. A 450 nm semiconductor laser was used to illuminate the top cladding layer of the devices to provide a pure carrier injection profile [24]. Measurements were undertaken on several devices with different diameters and under different optical powers to ensure the reproducibility of the results. For the cladding layer doping in these structures, the depletion edge moves towards the top surface by 30–45 nm between 0 V and breakdown voltage, resulting in a small increase in the primary photocurrent. The multiplication gain was determined from the photocurrent after accounting for this increasing primary photocurrent using the technique advocated by Woods *et al.* [25]. Although these changes are small, they can have a significant effect on the very low values of multiplication. These gain results are plotted as log (M – 1) verse reverse bias to show the full range of multiplication obtained in Fig. 1. The impact ionization coefficients were extracted from the gain curves using an iterative numerical technique [17]–[19] and based on an accurate knowledge of the electric field profiles in the range of structures investigated (including the background doping in the intrinsic region and depletion into the doped cladding layers). The impact ionization coefficients were assumed to be functions only of the electric field in the structures, and starting with the impact ionization coefficients of AlAsSb [26], the coefficients were adjusted until they gave good agreement with the experimentally measured multiplication characteristics.

These impact ionization coefficients for electrons and holes are shown in Fig. 2. The pure electron (p$^+$-i-n$^+$) and hole (n$^+$-i-p$^+$) initiated multiplication gains were simulated using these impact ionization coefficients and a random path length (RPL) model [17]–[19] for all the eight structures. As shown in Fig. 1, a good agreement is obtained between the measured and simulated gain curves over three orders of magnitude. The corresponding analytical expressions cover a wide electric field range from 260–1000 kV/cm for impact ionization coefficients of electrons and 200–1000 kV/cm for impact ionization coefficients of holes, and they are given by

$$\alpha = \begin{cases} 5.5 \times 10^5 \exp\left(-\left(\frac{1.21\times10^6}{E}\right)^{1.43}\right) \ \mathrm{cm}^{-1}, \\ \qquad \text{when } 260 \text{ kV/cm} < E < 500 \text{ kV/cm} \\ 8.0 \times 10^5 \exp\left(-\left(\frac{1.30\times10^6}{E}\right)^{1.43}\right) \ \mathrm{cm}^{-1}, \\ \qquad \text{when } 500 \text{ kV/cm} < E < 1000 \text{ kV/cm} \end{cases}, \quad (4)$$

$$\beta = \begin{cases} 2.5 \times 10^5 \exp\left(-\left(\frac{1.70\times10^6}{E}\right)^{1.44}\right) \ \mathrm{cm}^{-1}, \\ \qquad \text{when } 200 \text{ kV/cm} < E < 500 \text{ kV/cm} \\ 4.5 \times 10^5 \exp\left(-\left(\frac{1.92\times10^6}{E}\right)^{1.38}\right) \ \mathrm{cm}^{-1}, \\ \qquad \text{when } 500 \text{ kV/cm} < E < 1000 \text{ kV/cm} \end{cases}, \quad (5)$$

where E is the electric field in kV/cm.

The impact ionization coefficients of electrons in AlGaAsSb were found to be similar to AlAsSb except at very high electric fields (>500 kV/cm) as shown in Fig. 2. The bandgap changes slightly from AlAsSb to AlGaAsSb, with the X-valley bandgap changing from 1.64 eV to 1.56 eV and the Γ-valley bandgap changing from 1.95 eV to 1.77 eV [11]. This explains the similar impact ionization coefficients of electrons to AlAsSb but not the larger hole impact ionization coefficients. Similar behavior has been reported in $Al_xGa_{1-x}As$ and $(Al_xGa_{1-x})_{0.52}In_{0.48}P$ lattice-matched to GaAs [18], and for high Al composition, the breakdown voltage and impact ionization coefficients do not change much with Al variations. Fig. 2 shows that the α in AlGaAsSb is not only similar to that of AlAsSb [26] over much of the electric field range but also similar to α seen in InAlAs [28] and InP [29] (not shown for clarity). While the α at a typical electric field of 350 kV/cm in these four semiconductors is effectively identical at 1648 cm^{-1}, β shows orders of magnitude difference with β = 3300 cm^{-1} in InP, 167 cm^{-1} in InAlAs, 19 cm^{-1} in AlGaAsSb and 1.5 cm^{-1} in AlAsSb.

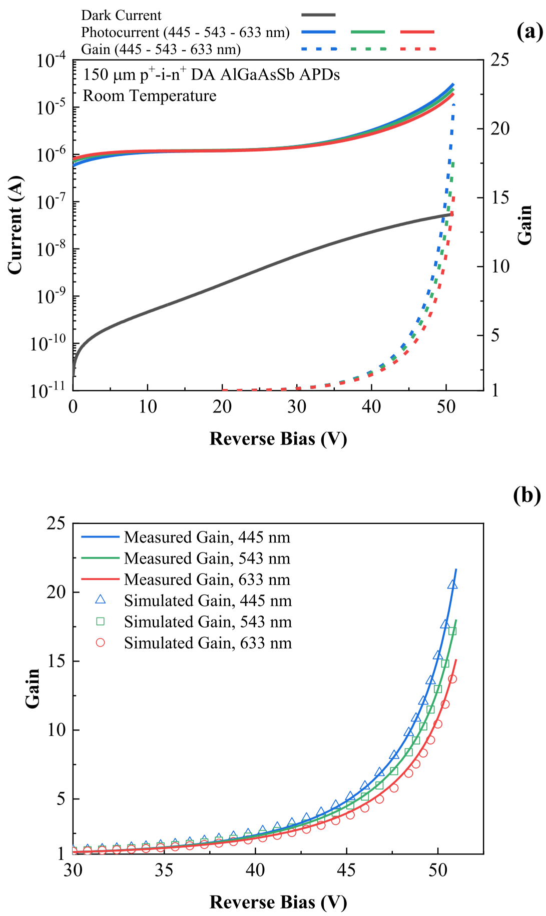

Fig. 3. (a) Dark current, photocurrent, and gain under 445, 543, 633 nm illumination for a 150-μm-diameter p$^+$-i-n$^+$ digital alloy AlGaAsSb APD with the 890-nm multiplication layer at room temperature. (b) Comparison between measured gain curves (solid lines) and simulated gain curves (points) based on the mixed injection method.

B. Mixed Injection Method

Determining the impact ionization coefficients of electrons and holes from multiplication gain under a pure electron injection profile (M_e) and under a pure hole injection profile (M_h) taken on different p$^+$-i-n$^+$ and n$^+$-i-p$^+$ structures respectively has the risk that small changes in the electric field profiles in the structures or the Al:Ga composition can introduce errors. Therefore, as a check, mixed injection [22] was employed to initiate the multiplication by both electrons and holes in the same structure and thereby extract the impact ionization coefficients for the digital alloy AlGaAsSb APD with the 890-nm multiplication layer. The only requirement with this technique is the accurate knowledge of absorption coefficients of this material. A similar technique was used to obtain the gain characteristics as described before. In order to obtain pure electron injection and mixed injection profiles, the light sources included a semiconductor laser to provide the 445 nm illumination and a He-Ne laser to provide the 543 and 633 nm illumination. Multiplication gain under three different carrier injection profiles were then calculated from the photocurrent, as shown in Fig. 3(a). With the illumination wavelength increasing, the pure electron injection

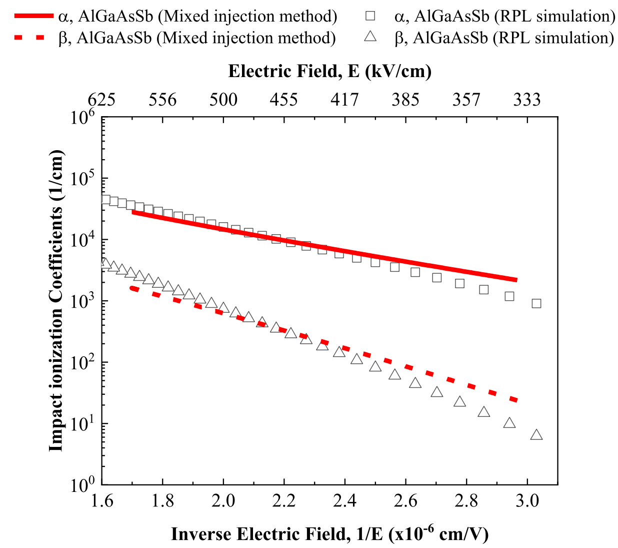

Fig. 4. Comparison of impact ionization coefficients of electrons and holes for AlGaAsSb extracted by the mixed injection method and by the random path length simulation.

profile transitions to the mixed injection profile, and a lower gain is obtained, an indication that the impact ionization coefficients of holes (β) are lower than those of electrons (α) [26].

The gain for an electron-hole pair created at position x of an ideal p$^+$-i-n$^+$ APD can be expressed by the local field model as [30]

$$M(x) = \frac{(\alpha - \beta)\, e^{-(\alpha-\beta)x}}{\alpha e^{-(\alpha-\beta)w} - \beta}, \tag{6}$$

where w is the depletion width. Combining the injection profile with the location-dependent gain, the mixed injection multiplication M_{mix} is expressed by [22]

$$M_{\text{mix}} = \frac{\int_0^w M(x)\, G(x)\, dx}{\int_0^w G(x)\, dx}, \tag{7}$$

$$G(x) \propto e^{-\gamma x}, \tag{8}$$

where $G(x)$ is the carrier-generation rate, and γ is the absorption coefficient. The absorption coefficients of AlGaAsSb were extracted via ellipsometry and verified by external quantum efficiency (EQE) measurements [24]. This mixed injection method has been used to extract the impact ionization coefficients for $In_{0.53}Ga_{0.47}As$ [22], $Al_{0.7}In_{0.3}As_{0.3}Sb_{0.7}$ [31], and $Al_{0.8}In_{0.2}As_{0.23}Sb_{0.77}$ [32].

By inserting the absorption coefficients of every layer and the measured gain curves into (7), the impact ionization coefficients of electrons and holes can be extracted [31], [32], and the simulated gain curves agree well with measured gain curves under 445, 543, and 633 nm illumination as shown in Fig. 3(b). Then, the impact ionization coefficients of electrons and holes extracted from two different methods are compared in Fig. 4. These two results of impact ionization coefficients agree well, with the small difference seen possibly due to the assumption of a constant electric field profile in the multiplication region in the mixed injection analysis. Mixed injection measurements were also undertaken on the 890-nm DA n^+-i-p^+ and 1020-nm RA p^+-i-n^+ structures which gave results that could be accurately replicated by the impact ionization coefficients that were derived.

IV. Discussion

As shown in Fig. 2, a large impact ionization coefficient ratio has been obtained for the $Al_xGa_{1-x}As_ySb_{1-y}$ material system, and while the electron ionization coefficients are similar to other materials like InAlAs, the hole ionization coefficient appears to be significantly reduced. This reduction in hole ionization coefficient may however be due to the antimonide (Sb) content. Generally in a semiconductor at high electric fields, holes gain energy and scatter from the heavier heavy/light-hole bands to the lighter split-off band from where they rapidly gain energy until they ionize. The heavier group V Sb atom has high spin-orbit coupling which pushes down the split-off band in the alloy band structure deeper into the valence band. This leads to an increase in the valence band spin-orbit splitting energy (Δ_{so}) [33]. Holes in the heavy/light hole bands may now reach the Brillouin zone edge and not be able to scatter into the split-off band, consequently the hole impact ionization rate is significantly reduced. This creates a large asymmetry between the electron and hole ionization coefficients, leading to a lower value of *k*. It has been showed recently in GaAsBi, which also has strong spin-orbit coupling due to the heavy Bi atom, that the increased Δso makes it harder for holes to scatter from the heavy/light-hole bands into the split-off band where their ionization threshold is gained [34], hence reducing the hole ionization coefficients.

This work also suggests that there is no obvious difference in impact ionization coefficients between digital alloy and random alloy AlGaAsSb, which is different from the previous report of impact ionization coefficients for InAlAs [35]. Both types of AlGaAsSb alloy contain the heavy Sb atoms which leads to a large Δso. For the AlGaAsSb system, we have a Δso of 0.5 eV for the random alloy and 0.44 eV for the digital alloy [33]. The Δso of this quaternary alloy is much larger than that of other non-Sb containing alloys (e.g., InP, InAlAs). The slightly smaller value for Δso in the digital alloy may be compensated for by the presence of small minigaps [36] in these periodic structures that localize holes and prevent hole impact ionization from occurring. As a result, the two alloy types may effectively have similar hole ionization coefficients.

It is interesting to note that the impact ionization coefficients given by (4) and (5) appear to be capable of replicating the avalanche multiplication in all the devices studied as shown in Fig. 2, even those with very narrow avalanche widths. Fig. 5, plotted so as to expand the voltage axis at low values, however shows that for the two thinnest p^+-i-n^+ structures, the local model actually overestimates the electron initiated multiplication at low values of multiplication. This is a clear indication that the "dead-space", the minimum distance cool carriers injected into the avalanche region need to travel to be in equilibrium with the high electric field, is suppressing the onset of electron impact ionization at low biases in very thin structures as observed in other materials like AlGaAs [37] and InAlAs [28]. This effect

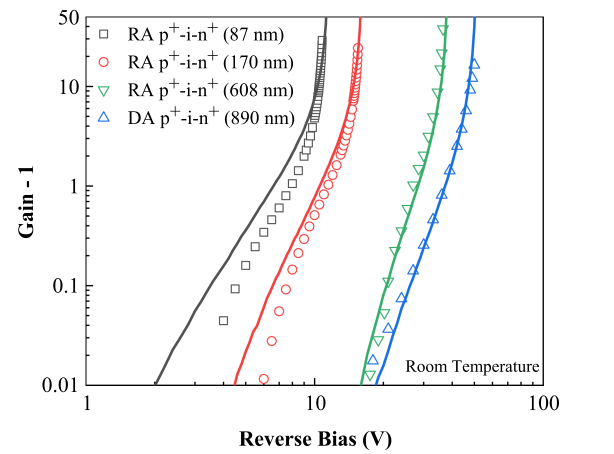

Fig. 5. Measured (symbols) and simulated gain curves (solid lines) from the random path length model for four p^+-i-n^+ AlGaAsSb APDs plotted on a log voltage axis to enhance the low voltages. (The data is from Fig. 1.).

is strongest in the thinnest p^+-i-n^+ structure and is negligible by the time the avalanche region width is ~600 nm or larger. A more in-depth analysis of the validity of the local model in the determination of avalanche multiplication was undertaken by Plimmer *et al.* [38] on GaAs p^+-i-n^+ structures, where experimental measurements were compared to local and Monte Carlo models. The results showed that the local model worked well for the i-region thicknesses greater than 200 nm.

V. Conclusion

The gain characteristics under different injection profiles have been investigated for digital alloy and random alloy AlGaAsSb APDs with different multiplication layer thickness in p^+-i-n^+ and n^+-i-p^+ structures. The impact ionization coefficients of electrons and holes have been determined from multiplication gain curves obtained with pure carrier injection profiles and by also employing a mixed injection method to independently extract the impact ionization coefficients. Both approaches gave effectively identical results. No discernable difference could be seen between the impact ionization coefficients of the structures grown as digital alloys and those grown as random alloys. The results show that the α in AlGaAsSb (85%) is identical to that of AlAsSb for electric fields up to 500 kV/cm while the β is larger, especially at low electric fields. The parameterized impact ionization coefficients are capable of replicating the multiplication characteristics of avalanching widths down ~600 nm, but for structures that are <200 nm, corrections for the "dead-space" are required to accurately predict the low values of electron multiplication.

References

[1] J. C. Campbell, "Recent advances in avalanche photodiodes," *J. Lightw. Technol.*, vol. 34, no. 2, pp. 278–285, 2016.

[2] J. C. Campbell, "Evolution of low-noise avalanche photodetectors," *IEEE J. Sel. Topics Quantum Electron.*, vol. 28, no. 2, Mar./Apr. 2021, Art. no. 3800911.

[3] J. C. Campbell, "Advances in photodetectors," in *Optical Fiber Telecommunications VA*, New York, NY, USA: Academic Press, 2008, pp. 221–268.

[4] B. E. A. Saleh and M. C. Teich, *Fundamentals of Photonics*, Hoboken, NJ, USA: Wiley, 2019.

[5] R. J. McIntyre, "Multiplication noise in uniform avalanche diodes," *IEEE Trans. Electron Devices*, vol. ED-13, no. 1, pp. 164–168, Jan. 1966.

[6] C. A. Lee, R. A. Logan, R. L. Batdorf, J. J. Kleimack, and W. Wiegmann, "Ionization rates of holes and electrons in silicon," *Phys. Rev.*, vol. 134, no. 3A, 1964, Art. no. A761.

[7] V. M. Robbins, T. Wang, K. F. Brennan, K. Hess, and G. E. Stillman, "Electron and hole impact ionization coefficients in (100) and in (111) Si," *J. Appl. Phys.*, vol. 58, no. 12, pp. 4614–4617, 1985.

[8] M. Ren, S. J. Maddox, M. E. Woodson, Y. Chen, S. R. Bank, and J. C. Campbell, "Characteristics of $Al_xIn_{1-x}As_ySb_{1-y}$ (x: 0.3∼0.7) avalanche photodiodes," *J. Lightw. Technol.*, vol. 35, no. 12, pp. 2380–2384, 2017.

[9] S. H. Kodati *et al.*, "AlInAsSb avalanche photodiodes on InP substrates," *Appl. Phys. Lett.*, vol. 118, no. 9, 2021, Art. no. 091101.

[10] X. Yi *et al.*, "Extremely low excess noise and high sensitivity $AlAs_{0.56}Sb_{0.44}$ avalanche photodiodes," *Nature Photon.*, vol. 13, no. 10, pp. 683–686, 2019.

[11] X. Zhou, S. Zhang, J. P. R. David, J. S. Ng, and C. H. Tan, "Avalanche breakdown characteristics of $Al_{1-x}Ga_xAs_{0.56}Sb_{0.44}$ quaternary alloys," *IEEE Photon. Technol. Lett.*, vol. 28, no. 22, pp. 2495–2498, Nov. 2016.

[12] X. Zhou, L. L. G. Pinel, S. J. Dimler, S. Zhang, J. S. Ng, and C. H. Tan, "Thin $Al_{1-x}Ga_xAs_{0.56}Sb_{0.44}$ diodes with low excess noise," *IEEE J. Sel. Topics Quantum Electron.*, vol. 24, no. 2, pp. 1–5, Feb. 2017.

[13] L. L. G. Pinel *et al.*, "Effects of carrier injection profile on low noise thin $Al_{0.85}Ga_{0.15}As_{0.56}Sb_{0.44}$ avalanche photodiodes," *Opt. Exp.*, vol. 26, no. 3, pp. 3568–3576, 2018.

[14] S. Lee *et al.*, "Low noise $Al_{0.85}Ga_{0.15}As_{0.56}Sb_{0.44}$ avalanche photodiodes on InP substrates," *Appl. Phys. Lett.*, vol. 118, no. 8, 2021, Art. no. 081106.

[15] J. Taylor-Mew, V. Shulyak, B. White, C. H. Tan, and J. S. Ng, "Low excess noise of $Al_{0.85}Ga_{0.15}As_{0.56}Sb_{0.44}$ avalanche photodiode from pure electron injection," *IEEE Photon. Technol. Lett.*, vol. 33, no. 20, pp. 1155–1158, Oct. 2021.

[16] S. Lee *et al.*, "Random alloy thick AlGaAsSb avalanche photodiodes on InP substrates," *Appl. Phys. Lett.*, vol. 120, no. 7, 2022, Art. no. 071101.

[17] D. S. Ong, K. F. Li, G. J. Rees, J. P. R. David, and P. N. Robson, "A simple model to determine multiplication and noise in avalanche photodiodes," *J. Appl. Phys.*, vol. 83, no. 6, pp. 3426–3428, 1998.

[18] H. I. J. Lewis *et al.*, "Impact ionization coefficients in $(Al_xGa_{1-x})_{0.52}In_{0.48}P$ and $Al_xGa_{1-x}As$ lattice-matched to GaAs," *IEEE Trans. Electron Devices*, vol. 68, no. 8, pp. 4045–4050, Aug. 2021.

[19] X. Jin *et al.*, "Temperature dependence of the impact ionization coefficients in AlAsSb lattice matched to InP," *IEEE J. Sel. Topics Quantum Electron.*, vol. 28, no. 2, pp. 1–8, Mar./Apr. 2021.

[20] M. M. Hayat, B. E. A. Saleh, and M. C. Teich, "Effect of dead space on gain and noise of double-carrier-multiplication avalanche photodiodes," *IEEE Trans. Electron Devices*, vol. 39, no. 3, pp. 546–552, Mar. 1992.

[21] R. J. McIntyre, "A new look at impact ionization-Part I: A theory of gain, noise, breakdown probability, and frequency response," *IEEE Trans. Electron Devices*, vol. 46, no. 8, pp. 1623–1631, Aug. 1999.

[22] J. S. Ng, C. H. Tan, J. P. R. David, G. Hill, and G. J. Rees, "Field dependence of impact ionization coefficients in $In_{0.53}Ga_{0.47}As$," *IEEE Trans. Electron Devices*, vol. 50, no. 4, pp. 901–905, Apr. 2003.

[23] S. Xie *et al.*, "InGaAs/AlGaAsSb avalanche photodiode with high gain-bandwidth product," *Opt. Exp.*, vol. 24, no. 21, pp. 24242–24247, 2016.

[24] B. Guo *et al.*, "Optical constants of $Al_{0.85}Ga_{0.15}As_{0.56}Sb_{0.44}$ and $Al_{0.79}In_{0.21}As_{0.74}Sb_{0.26}$," *Appl. Phys. Lett.*, vol. 119, no. 17, 2021, Art. no. 171109.

[25] M. H. Woods, W. C. Johnson, and M. A. Lampert, "Use of a Schottky barrier to measure impact ionization coefficients in semiconductors," *Solid-State Electron.*, vol. 16, no. 3, pp. 381–394, 1973.

[26] X. Yi *et al.*, "Demonstration of large ionization coefficient ratio in $AlAs_{0.56}Sb_{0.44}$ lattice matched to InP," *Sci. Rep.*, vol. 8, no. 1, pp. 1–6, 2018.

[27] R. Van Overstraeten and H. De Man, "Measurement of the ionization rates in diffused silicon *p-n* junctions," *Solid-State Electron.*, vol. 13, no. 5, pp. 583–608, 1970.

[28] Y. L. Goh *et al.*, "Avalanche multiplication in InAlAs," *IEEE Trans. Electron Devices*, vol. 54, no. 1, pp. 11–16, Jan. 2007.

[29] L. J. J. Tan, J. S. Ng, C. H. Tan, and J. P. R. David, "Avalanche noise characteristics in submicron InP diodes," *IEEE J. Quantum Electron.*, vol. 44, no. 4, pp. 378–382, Apr. 2008.

[30] G. E. Stillman and C. M. Wolfe, "Avalanche photodiodes," in *Semiconductors and Semimetals*. vol. 12. Amsterdam, The Netherlands; New York, NY, USA: Elsevier, 1977, pp. 330–337.

[31] Y. Yuan, J. Zheng, A. K. Rockwell, S. D. March, S. R. Bank, and J. C. Campbell, "AlInAsSb impact ionization coefficients," *IEEE Photon. Technol. Lett.*, vol. 31, no. 4, pp. 315–318, Feb. 2019.

[32] A. H. Jones, A. K. Rockwell, S. D. March, Y. Yuan, S. R. Bank, and J. C. Campbell, "High gain, low dark current $Al_{0.8}In_{0.2}As_{0.23}Sb_{0.77}$ avalanche photodiodes," *IEEE Photon. Technol. Lett.*, vol. 31, no. 24, pp. 1948–1951, Dec. 2019.

[33] S. Z. Ahmed, "A multiscale study of P-I-N devices for computing and sensing applications," Ph.D. dissertation, Sch. Eng. App. Sci., Univ. of Virginia, Charlottesville, VA, USA, 2021.

[34] Y. Liu *et al.*, "Valence band engineering of GaAsBi for low noise avalanche photodiodes," *Nature Commun.*, vol. 12, no. 1, pp. 1–8, 2021.

[35] Y. Yuan *et al.*, "Temperature dependence of the ionization coefficients of InAlAs and AlGaAs digital alloys," *Photon. Res.*, vol. 6, no. 8, pp. 794–799, 2018.

[36] J. Zheng *et al.*, "Digital alloy InAlAs avalanche photodiodes," *J. Lightw. Technol.*, vol. 36, no. 17, pp. 3580–3585, 2018.

[37] B. K. Ng *et al.*, "Avalanche multiplication characteristics of $Al_{0.8}Ga_{0.2}As$ diodes," *IEEE Trans. Electron Devices*, vol. 48, no. 10, pp. 2198–2204, Oct. 2001.

[38] S. A. Plimmer, J. P. R. David, and D. S. Ong, "The merits and limitations of local impact ionization theory," *IEEE Trans. Electron Devices*, vol. 47, no. 5, pp. 1080–1088, May 2000.

Bingtian Guo received the B.S. degree in opto-electronics information science and engineering from Nankai University, Nankai, China, in 2019. He is currently working toward the Ph.D. degree in electrical engineering with the University of Virginia, Charlottesville, VA, USA. His research interests include high-power and high-speed photodiodes.

Xiao Jin received the B.Eng. degree in electronic electrical engineering in 2018 from The University of Sheffield, Sheffield, U.K., where he is currently working toward the Ph.D. degree with Semiconductor Group. The aim of his Ph.D. research is to develop APDs capable of operating at very high speeds and high sensitivity for next generation telecommunication networks. He is studying the impact ionization process via different modeling techniques and look experimentally at the ionization coefficient in different semiconductor materials and device structures. His research interests include the characterization of III-V semiconductor material and devices, especially that AlAsSb/AlGaAsSb material systems.

Seunghyun Lee received the M.Eng. degree in 2021 from The Ohio State University, Columbus, OH, USA, where he is currently working toward the Ph.D. degree in electrical and computer engineering. His research interests include the development of high-sensitivity and high-speed avalanche photodiodes for telecommunication networks and light detection and ranging systems. His specific research interest include growing extremely low impurity materials and designing a novel device structure for various device applications.

Sheikh Z. Ahmed received the B.Sc. degree from BRAC University, Dhaka, Bangladesh, and the Ph.D. degree from the University of Virginia, Charlottesville, VA, USA. He is currently with Intel Corporation. His research interests include the computational study of nanoelectronic and photonic devices, analytical modeling, quantum transport, and compact modeling.

Andrew H. Jones received the B.S. degree in electrical engineering from Grove City College, Grove City, PA, USA, and the Ph.D. degree in electrical engineering from the University of Virginia, Charlottesville, VA, USA. He w a Navy Contractor for two years in Pittsburgh, PA, USA. He is currently a Postdoc with the Department of Electrical and Computer Engineering, University of Virginia. His research interests include photonic devices, specifically the design and fabrication of avalanche photodiodes for visible and infrared applications.

Xingjun Xue received the B.E. degree in electronic and information engineering from Xidian University, Xi'an, China, in 2013, and the Ph.D. degree in electronic science and technology from Tsinghua University, Beijing, China, in 2019. She is currently a Research Associate with the Department of Electrical and Computer Engineering, University of Virginia, Charlottesville, VA, USA. Her research interests include the design, fabrication, and characterization of avalanche photodiode.

Baolai Liang received the Ph.D. degree in microelectronics-photonics from the University of Arkansas, Fayetteville, AR, USA. He is currently the Director of the Integrated Nanomaterials Laboratory, California NanoSystems Institute, University of California, Los Angeles, Los Angeles, CA, USA. His research interests include molecular beam epitaxy growth and optical characterizations of low-dimensional III-V semiconductor materials for optoelectronics device application.

Harry I. J. Lewis received the M.Eng. degree in 2018 from the University of Sheffield, Sheffield, U.K., where he is currently working toward the Ph.D. degree with the Impact Ionization Group. His research interests include impact ionization in III-V semiconductors, with a focus on the measurement and characterization of excess noise and the development of low-noise APDs, and low-noise analogue circuitry.

Sri H. Kodati received the master's degree from the University of Missouri-Kansas City, Kansas City, MO, USA, in 2016. He is currently working toward the Ph.D. degree with the Department of Electrical and Computer Engineering, The Ohio State University, Columbus, OH, USA. His research interests include develop low-cost and highly sensitive detectors for optical communications and light detection and ranging (LiDAR) applications, to replace commercial technologies. His research interests also includedesign, modeling, fabrication, and analysis of III-V detectors employing vertical and lateral architectures.

Dekang Chen received the bachelor's degree in mechanical engineering from the Hefei University of Technology, Hefei, China, in 2016, and the master's degree in optical engineering from the University of Science and Technology of China, Hefei, China, in 2019. He is currently working toward the Ph.D. degree with Prof. Joe Campbell's Group, ECE Department. His research interests include photonic device simulation and testing, especially high-performance avalanche photodetectors.

Theodore J. Ronningen received the Ph.D. in chemical physics from The Ohio State University, Columbus, OH, USA. He is currently a Research Scientist with the Department of Electrical and Computer Engineering, The Ohio State University. He was a Senior Research Scientist with Battelle, developing products and processes to improve the detection of hazardous materials for defense and security applications. He has been awarded ten patents. At Ohio State, he supports two university-wide initiatives, NSF NeXUS Facility, and IIT Bombay-Ohio State Frontier Center. He is the Chair of the Out To Innovate Professional Society.

Christoph H. Grein received the Ph.D. degree in theoretical condensed matter physics from Princeton University, Princeton, NJ, USA. He is currently a Professor with the Department of Physics, University of Illinois at Chicago, Chicago, IL, USA. He held Postdoctoral Fellowships with the Max Planck Institute, Stuttgart, Germany, and with Harvard University, Cambridge, MA, USA, before joining the University of Illinois, Champaign, IL, USA. He has more than 225 peer-reviewed journal articles, eight issued patents and several keynote and invited talks. He is also an Associate Editor for the journal *Applied Physics Letters*. He is a Fellow of the American Physical Society and a Fellow of SPIE.

Avik W. Ghosh (Senior Member) received the Ph.D. degree in physics from The Ohio State University, Columbus, OH, USA. He did Postdoctoral Fellowship in electrical engineering with Purdue University, West Lafayette, IN, USA. He is currently a Professor of electrical and computer engineering and Professor of physics with the University of Virginia, Charlottesville, VA, USA. He has more than 100 refereed papers and book chapters and two upcoming books in the areas of computational nano-electronics and low power devices, specializing in materials to systems modeling (DFT2SPICE), including 2D materials, thin films for photodetectors, molecular electronics, subthermal switching, nanomagnetic materials and devices, and nanoscale heat flow. He is a Fellow of the Institute of Physics (IOP). He was the recipient of the IBM Faculty Award, NSF CAREER Award, a Best Paper Award from the Army Research Office, Charles Brown New Faculty Teaching Award, and All-University Teaching Award.

Sanjay Krishna (Fellow, IEEE) received the M.S. degree in electrical engineering and the Ph.D. degree in applied physics from the University of Michigan, Ann Arbor, MI, USA. He is currently the George R Smith Professor of engineering with the Department of ECE, The Ohio State University, Columbus, OH, USA. Then, he joined The University of New Mexico, Albuquerque, NM, USA, as a Tenure Track Faculty Member. He is also a Visiting Faculty with the Indian Institute of Technology, Mumbai, India. He has more than 300 peer-reviewed journal articles (h-index = 59), ten issued patents, and several keynote and invited talks. He was the recipient of several awards, including the Gold Medal from the Indian Institute of Technology, Madras, Defense Intelligence Agency Chief Scientist Award for Excellence, SPIE Technology Achievement Award, IEEE Aron Kressel Award, and the UNM Teacher of the Year award. He is the co-founder and CTO of SK Infrared, a start-up involved with the use of IR imaging for defense and commercial applications. He is a Fellow of OSA and SPIE.

John P. R. David (Fellow, IEEE) received the B.Eng. degree in electronic engineering and the Ph.D. degree from The University of Sheffield, Sheffield, U.K., in 1979 and 1983, respectively. From 1982 to 2001, he was a Postdoctoral Researcher with The University of Sheffield, on the study of impact ionization coefficients and III-V materials characterization. From 2001 to 2002, he was a Senior Engineer with Bookham Technologies, before returning to The University of Sheffield, as a Senior Lecturer. He has authored or coauthored more than 350 journal articles and has more than 350 conference presentations, in the areas of avalanche photodiodes, impact ionization, and III-Material characterization. From 2002 to 2004, he was an IEEE LEOS Distinguished Lecturer, giving presentations on the topic of LowNoiseAvalanche Photodiodes. He is a Fellow of IET.

Joe C. Campbell (Life Fellow, IEEE) received the B.S. degree in physics from the University of Texas at Austin, Austin, TX, USA, in 1969, and the M.S. and Ph.D. degrees in physics from the University of Illinois at Urbana-Champaign, Champaign, IL, USA, in 1971 and 1973, respectively. From 1974 to 1976, he was employed with Texas Instruments where he worked on integrated optics. In 1976, he joined the Staff of AT&T Bell Laboratories in Holmdel, NJ, USA. He worked on a variety of optoelectronic devices, including semiconductor lasers, optical modulators, waveguide switches, photonic integrated circuits, and photodetectors with emphasis on high-speed avalanche photodiodes for high-bit-rate lightwave systems with Crawford Hill Laboratory. In January 1989, he joined the Faculty of the University of Texas at Austin, as a Professor of electrical and computer engineering and the Cockrell Family Regents Chair of engineering. In January 2006, he moved to the University of Virginia, Charlottesville, VA, USA, as the Lucian Carr Professor of electrical and computer engineering. He has coauthored 11 book chapters, 490 articles for refereed technical journals, and more than 500 conference presentations. His technical area is photodetectors. His research interests include single-photon-counting APDs, Si-based optoelectronics, high-speed low-noise avalanche photodiodes, and high-power high-linearity photodiodes. In 2002, he was inducted into the National Academy of Engineering.